

X-ray properties of power-law BzK galaxies

C. Feruglio (CEA), E. Daddi (CEA), F. Fiore (INAF), S. Puccetti (ASI), F. Civano (CfA), M. Elvis (CfA) et al. (COSMOS team)

We use the BzK catalog of galaxies to select candidate obscured AGN, not directly detected in X-rays in the *Chandra*-COSMOS survey (C-COSMOS), in the redshift range $z=1.5-3$, and study their X-ray properties by using stacking analysis. We find that the sources with power-law SEDs in the IRAC bands and without a direct detection in X-rays are detected in both the soft and hard bands in the *Chandra* stacked images. Their average spectrum is compatible with large obscuration ($N_H \geq 10^{24} \text{ cm}^{-2}$) and therefore we conclude that they are highly obscured AGN. We study their volume density, and find that this is consistent with the X-ray background model predictions for Compton thick AGN.

Sample selection

We select COSMOS BzK galaxies at $z=1.4-3$ with: a) power-law SED in the IRAC bands (as Donley et al. 2008) b) counts < 10 in 0.5-7 keV band in *Chandra*-COSMOS, c) expotime ≥ 200 ks, in order to study their X-ray properties using stacking of the *Chandra*-COSMOS data. Their average SED are shown in Fig. 1.

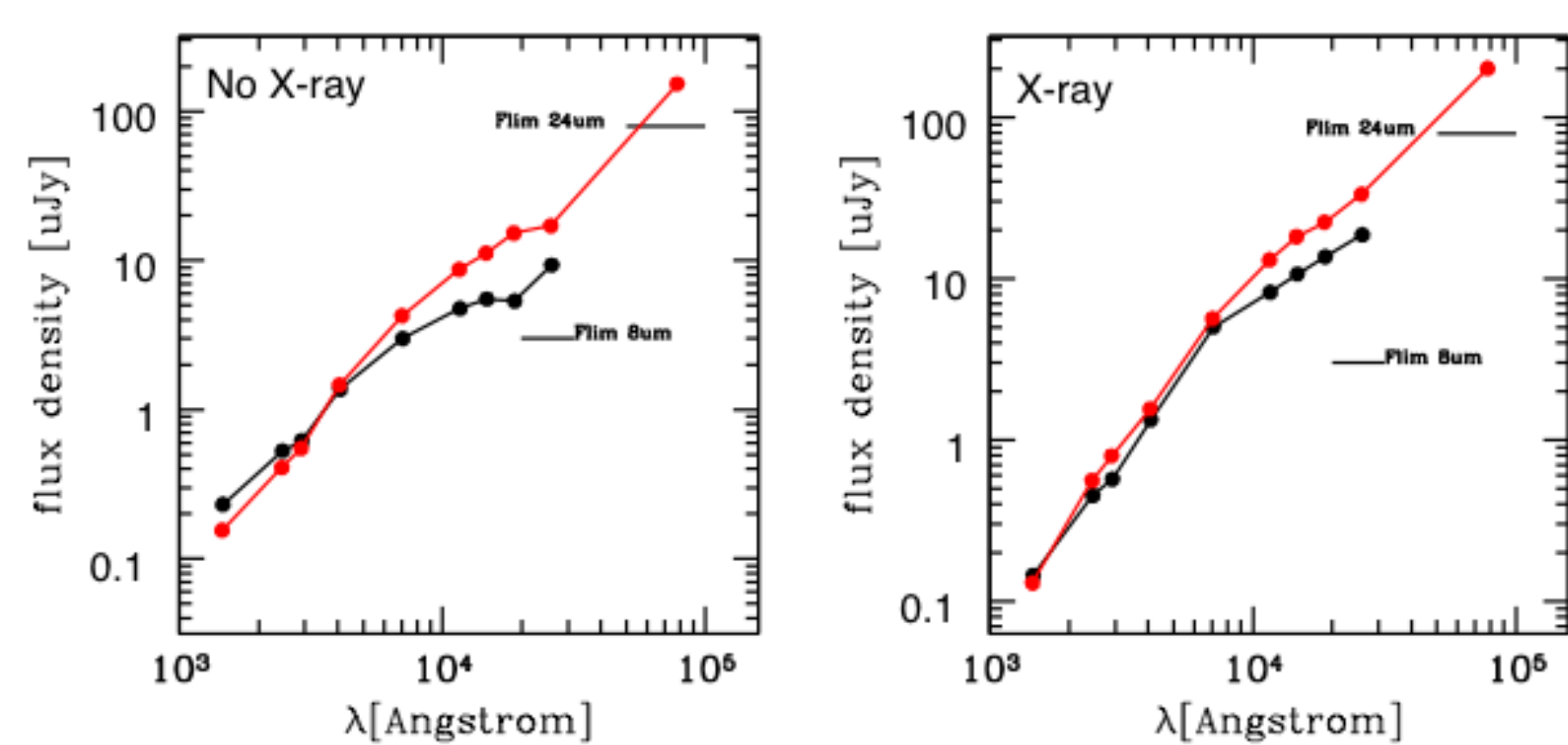


Fig. 1. Left: average SED of MIPS detected (red) and MIPS undetected (black) power-law sources without direct X-ray detection. Right panel: average SED of the BzK X-ray detected galaxies (i.e. AGN from Puccetti+2009, Elvis+2010, Civano+2010).

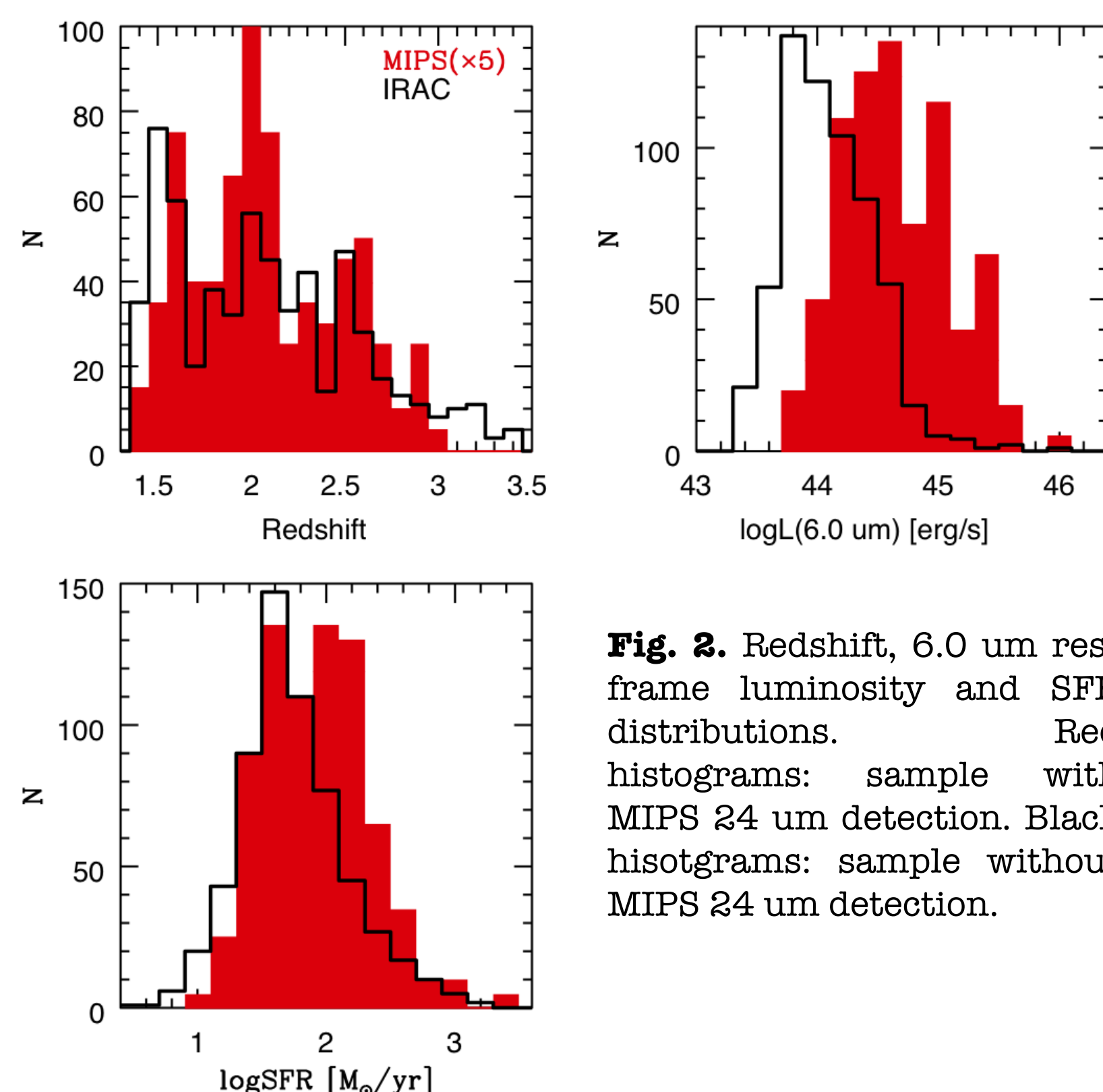


Fig. 2. Redshift, 6.0 um rest frame luminosity and SFR distributions. Red histograms: sample with MIPS 24 um detection. Black histograms: sample without MIPS 24 um detection.

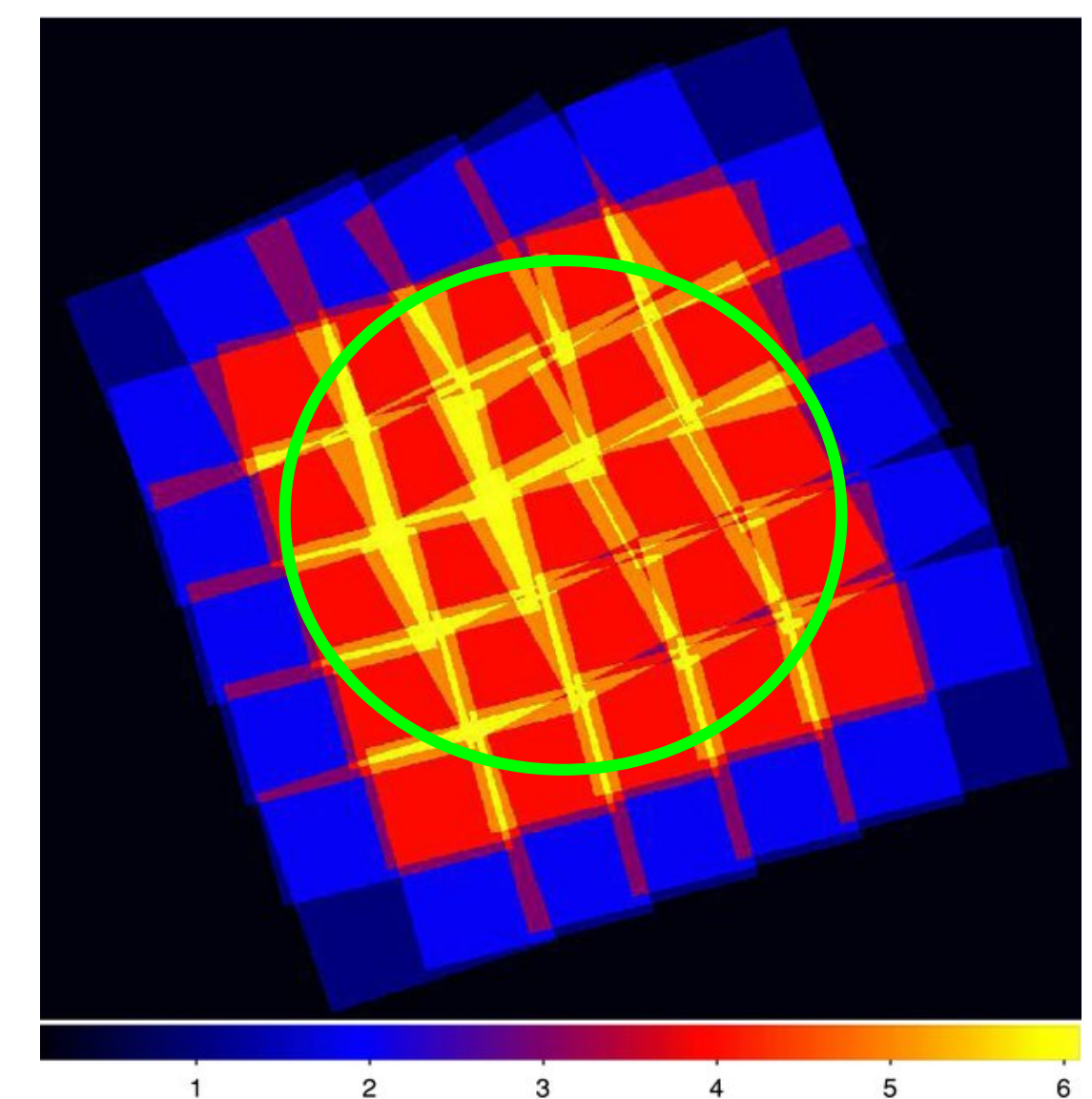


Fig. 3. *Chandra*-COSMOS tiling showing the area used in the stacking analysis, 0.45 sq deg (orange area, from Puccetti+2009)

X-ray stacking results

To study the X-ray properties of the power-law sources without a direct X-ray detection we performed a stacking analysis of the *Chandra* counts at the position of each source for the two samples. The *Chandra* deep and uniform coverage allows us to increase the sensitivity by factor of 100 using the stacking technique (Daddi et al. 2007, Fiore et al. 2008, 2009).

We stack in 3 observed energy bands: **0.3-1.5 keV**, **1.5-2.8 keV** and **2.8-7 keV**. These bands allow to probe the Fe K emission line at 1.5-2.8 keV for sources at $z \sim 2$ (median redshift of the samples).

Fig. 4 shows the stacked images and the average spectra obtained for the MIPS 24 um detected sample and the MIPS undetected sample.

Both samples are detected in all the 3 bands with a significance of > 5 sigma. They show a hard excess relative to the soft band (0.3-1.5 keV) flux, compared to a $\Gamma=1.9$ spectrum of pure star formation. Both samples are consistent with composite objects showing star formation plus a heavily obscured AGN. We notice that the shape of the average spectra might be due to the contribution of a few reflection-dominated sources in the sample.

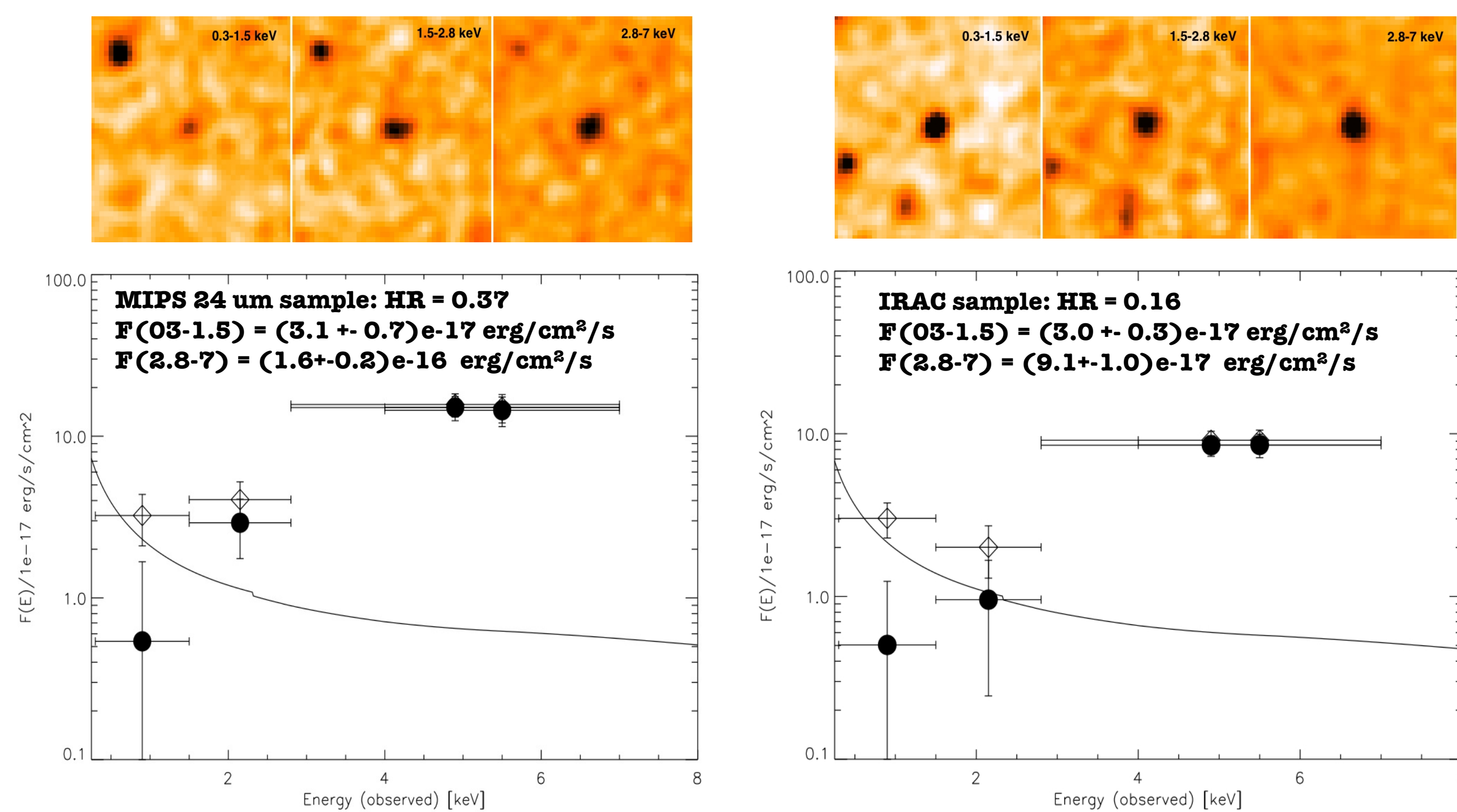


Fig. 4. Stacked images (top panels) and average spectra (lower panels, open symbols) of the MIPS 24 um power-law sample (left) and the MIPS undetected sample (right). Filled symbols show the average spectra after subtraction of the star-formation contribution in the 0.3-1.5 keV band. Solid line: $\Gamma=1.9$ spectrum of pure star formation.

Obscuration

In order to estimate N_H we fit these spectra with models (*photoelectric absorption* * (*powerlaw+gaussian component*)) and pure reflection above $\log N_H = 24.5 \text{ cm}^{-2}$.

We find the following column densities: $N_H = 24.9 (+0.8/-1) \text{ cm}^{-2}$ for the MIPS 24 um sample and $N_H = 24.7 (+0.2/-0.4) \text{ cm}^{-2}$ for the IRAC sample. In Fig. 5 we compare these values with the N_H obtained using observed $L(2-10 \text{ keV})$ (i.e. not corrected for absorption), $L(6\mu\text{m})_{\text{RF}}$, and model predictions.

We find: $N_H = 24.7 \pm 0.5 \text{ cm}^{-2}$ for the MIPS 24 um sources and $N_H = 24.1_{-0.2}^{+0.8} \text{ cm}^{-2}$ for the IRAC sources. These two independent estimates of the obscuration imply that these power-law SED sources host highly obscured AGN.

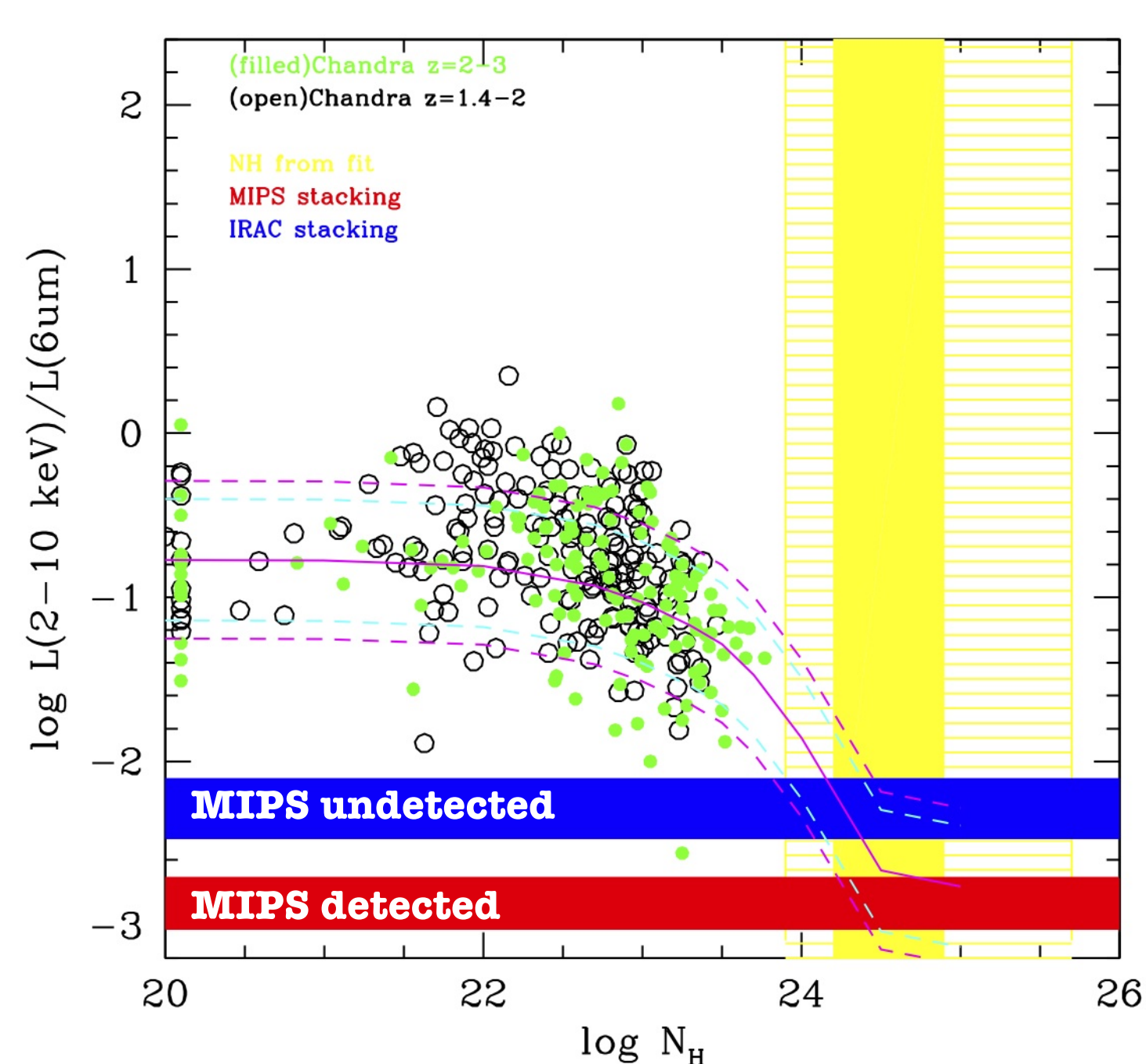


Fig. 5. The X-ray to infrared ratio vs. the column density. Black and green symbols show the sources individually detected in X-ray by *Chandra* in 2 redshift intervals. Yellow areas show the N_H estimated from spectral fitting for the 2 samples (Fig. 4). Red and blue areas show the ratio observed for the MIPS detected and undetected samples. The two N_H estimates agree with model predictions (magenta and cyan lines)

The Density of highly obscured AGN

We compute the space density of highly obscured AGN in bins of redshift and $L(2-10 \text{ keV})$ luminosity by using all the MIPS detected and MIPS undetected sources used in the stacking. In principle only a fraction of the stacked sources might contribute to the hard X-ray signal. However, given that all sources have a power law SED we assume that all of them hosts an AGN. The space density is shown in Fig. 6 and it is consistent with the Gilli et al. (2007) model predictions for Compton thick AGN.

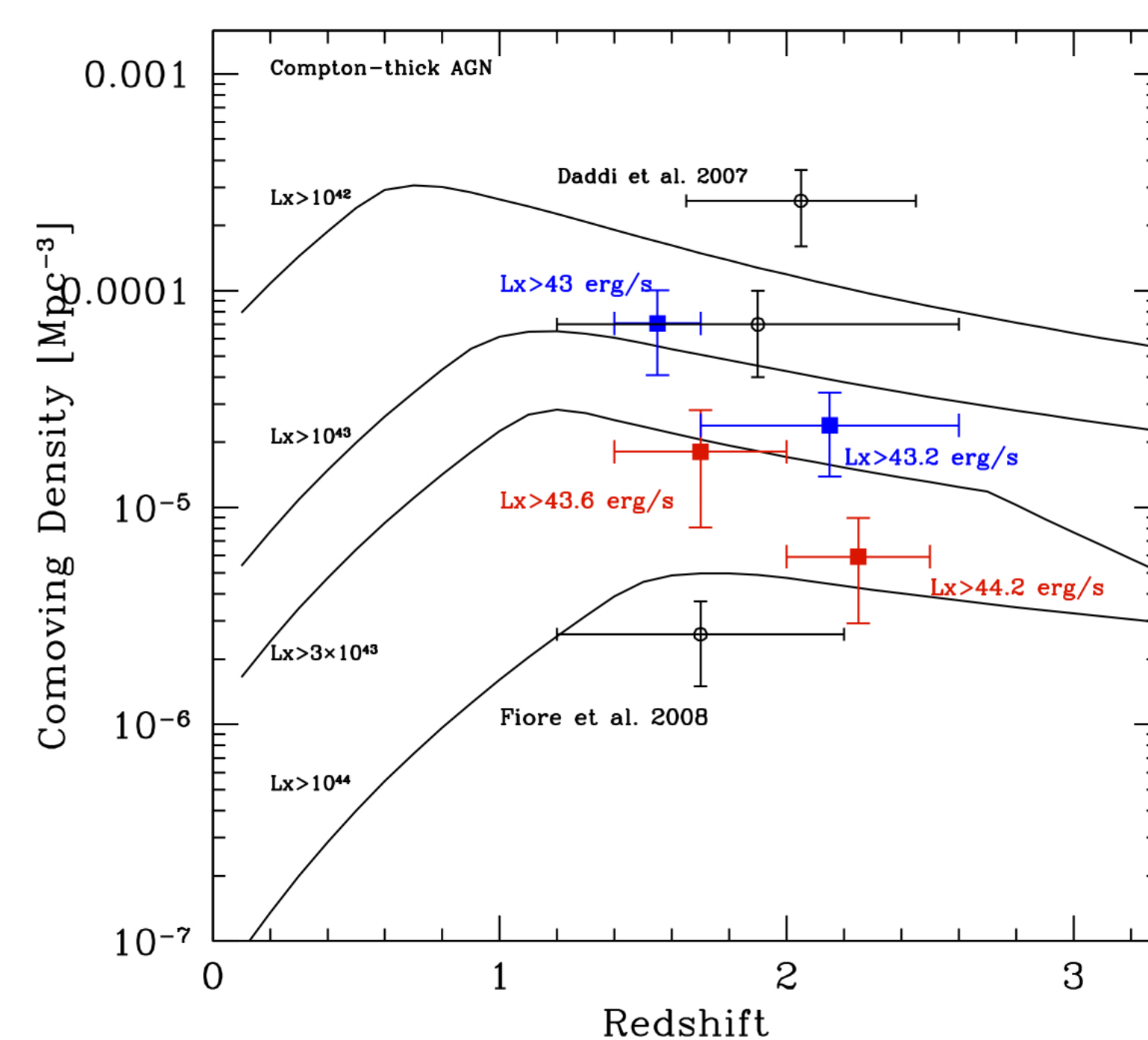


Fig. 6. Comoving density of highly obscured AGN in bins of redshift and $L(2-10 \text{ keV})$. Red symbols: MIPS 24 micron power-law sources used in the stacking. Blue symbols: MIPS undetected sources (we show also Daddi et al 2007 and Fiore et al. 2009 results, black points). Solid lines are the model expectations for $\log L(2-10 \text{ keV}) > 42, 43, 43.5, 44 \text{ erg/s}$ (Gilli et al. 2007).